

Excitation and photoionization processes involving the bound ns electrons

A.V. Nefiodov^{a,b,*} and G. Plunien^a

^a*Institut für Theoretische Physik, Technische Universität Dresden,
MommSENstraße 13, D-01062 Dresden, Germany*

^b*Petersburg Nuclear Physics Institute,
188300 Gatchina, St. Petersburg, Russia*

(Dated: Received February 1, 2008)

Abstract

We have considered the processes of excitation and ionization of light multicharged ions by impact of high-energy particles, which proceed with participation of the ns electrons. The screening corrections to the energy levels and photoionization cross sections are evaluated analytically within the framework of the non-relativistic perturbation theory with respect to the electron-electron interaction. The universal scalings for the excitation and ionization cross sections are studied for arbitrary principal quantum numbers n .

PACS numbers: 34.80.Kw; 32.80.Fb; 31.25.-v

*Corresponding author.

E-mail address: nefiodov@theory.phy.tu-dresden.de (A.V. Nefiodov).

1. Since decades the fundamental processes of excitation and ionization of few-electron atomic ions have been persistently investigated within the framework of different sophisticated approaches, due to necessity of the accurate account of all interactions in the colliding system (see, for example, the works [1, 2, 3, 4, 5, 6, 7] and references there). The deduction of the universal scaling behavior for differential and total cross sections is of particular importance, because it allows one to establish generic features of various processes for a wide family of targets [8, 9, 10, 11]. In this Letter, we study the excitation and photoionization of light multicharged ions, which proceed with participation of the ns electrons. As a method, the consistent non-relativistic perturbation theory in the Furry picture is employed [12]. The calculations are performed analytically, taking into account the one-photon exchange diagrams.

The characteristic quantities for the theoretical description of collision processes on multicharged ions are the Coulomb potential $I = \eta^2/(2m)$ for single ionization from the K shell, the average momentum $\eta = m\alpha Z$ of the K-shell electron, the Bohr radius $a_0 = 1/(m\alpha)$, the electron mass m , and the fine-structure constant α ($\hbar = 1$, $c = 1$). The parameter αZ is supposed to be sufficiently small ($\alpha Z \ll 1$), although we assume nuclear charges with $Z \gg 1$.

2. In the non-relativistic theory, the stationary states of hydrogen-like atomic system are characterized by the principal quantum number n , the value of angular momentum l , and projection of the orbital angular momentum m [13]. The corresponding eigenfunctions, which are solutions of the Schrödinger equation for a bound electron in the external Coulomb field of a point nucleus, read [14, 15]

$$\psi_{nlm}(\mathbf{r}) = R_{nl}(r)Y_{lm}(\theta, \varphi), \quad (1)$$

$$R_{nl}(r) = -2\eta_n^{3/2} \frac{\sqrt{(n-l-1)!}}{\sqrt{[(n+l)!]^3 n}} e^{-\eta_n r} (2\eta_n r)^l L_{n+l}^{2l+1}(2\eta_n r), \quad (2)$$

$$E_{nl} = -I_n = -\frac{I}{n^2}. \quad (3)$$

Here $\eta_n = \eta/n$ and Y_{lm} are the spherical harmonics. The wave functions are normalized in the standard fashion

$$\int d\mathbf{r} \psi_{nlm}^*(\mathbf{r}) \psi_{n'l'm'}(\mathbf{r}) = \delta_{nn'} \delta_{ll'} \delta_{mm'}, \quad (4)$$

$$\int_0^\infty dr r^2 R_{nl}(r) R_{n'l}(r) = \delta_{nn'}. \quad (5)$$

According to works [16, 17, 18], it is convenient to represent the associated Laguerre polynomials

in Eq. (2) via the contour integral

$$L_{n+l}^{2l+1}(\zeta) = -\frac{(n+l)!}{2\pi i} \oint^{(0+)} dt \frac{\exp[-\zeta t/(1-t)]}{(1-t)^{2l+2} t^{n-l}}, \quad (6)$$

where the closed path encircles counter-clockwise the origin $t = 0$, but not the point $t = 1$.

In the following, we shall focus on the bound ns states ($l = 0$). In the momentum representation, the corresponding eigenfunctions (1) can be written as

$$\psi_{ns}(\mathbf{f}) = \frac{1}{\sqrt{4\pi}} R_{n0}(f), \quad (7)$$

$$R_{n0}(f) = \frac{\sqrt{\eta_n}}{n} \frac{1}{2\pi i} \oint^{(\eta_n^+)} dy \frac{(y + \eta_n)^n}{(y - \eta_n)^n} \left(-\frac{\partial}{\partial \lambda} \right) \langle \mathbf{f} | V_{i\lambda} | 0 \rangle \Big|_{\lambda=y}, \quad (8)$$

$$\langle \mathbf{f}' | V_{i\lambda} | \mathbf{f} \rangle = \frac{4\pi}{(\mathbf{f}' - \mathbf{f})^2 + \lambda^2}. \quad (9)$$

In Eq. (8), after taking the derivative with respect to λ , one should set $\lambda = y$ and then perform the contour integration enclosing the pole at $y = \eta_n$.

3. Let us consider a helium-like ion in the pure ns^2 (1S) state. Within the framework of non-relativistic perturbation theory with respect to the electron-electron interaction, the energy levels E are given as a series in powers of the reversed nuclear charge Z^{-1}

$$E = E^{(0)} + \sum_{k \geq 1} \Delta E^{(k)} \equiv I \sum_{k \geq 0} \epsilon_k Z^{-k}, \quad (10)$$

where $\epsilon_0 = -2n^{-2}$. The dimensionless coefficients ϵ_k depend on the principal quantum number n .

The first-order correlation correction $\Delta E^{(1)}$ can be written as

$$\Delta E^{(1)} = 4\pi\alpha \int \frac{d\mathbf{f}}{(2\pi)^3} \frac{d\mathbf{f}_1}{(2\pi)^3} \frac{d\mathbf{f}_2}{(2\pi)^3} \langle \psi_{ns} | \mathbf{f}_1 \rangle \langle \mathbf{f}_1 + \mathbf{f} | \psi_{ns} \rangle \frac{1}{f^2} \langle \psi_{ns} | \mathbf{f}_2 \rangle \langle \mathbf{f}_2 - \mathbf{f} | \psi_{ns} \rangle. \quad (11)$$

Performing integrations over the intermediate momenta yields

$$\begin{aligned} \Delta E^{(1)} &= \alpha N_{ns} \frac{1}{2n^3} \frac{1}{(2\pi i)^3} \oint \prod_{k=1}^3 \left[dy_k \frac{(y_k + \eta_n)^n}{(y_k - \eta_n)^n} \right] \\ &\quad \times \left(-\frac{\partial}{\partial \lambda} \right) \frac{1}{\lambda^2} \langle \psi_{ns} | (V_{iy_3} - V_{i(\lambda+y_3)}) | 0 \rangle \Big|_{\lambda=y_1+y_2}, \end{aligned} \quad (12)$$

where $N_{ns}^2 = \eta_n^3/\pi$ and $\eta_n = \eta/n$. The matrix element evaluated with the Coulomb wave function (1) reads [19]

$$\langle \psi_{nlm} | V_{i\lambda} | 0 \rangle = 4\pi N_{ns} \frac{(\lambda - \eta_n)^{n-1}}{(\lambda + \eta_n)^{n+1}} \delta_{l0} \delta_{m0}. \quad (13)$$

The integrals in the expression (12) are given by residues of the integrand at the poles $y_k = \eta_n$, ($k = 1, 2, 3$). For the ground state ($n = 1$), $\epsilon_1 = 5/4$ [15], while for the $2s^2$ configuration, $\epsilon_1 = 77/256$ [20]. In Table I, we present the coefficients $\epsilon_1 = Z\Delta E^{(1)}/I$ calculated for the principal quantum numbers $n \leq 16$. In the asymptotic limit $n \gg 1$, $n^2\epsilon_1$ tends to the constant 1.189.

As another example, we shall also evaluate the correlation correction $\Delta E^{(1)}$ for helium-like ion in the $1sns$ ($^1, ^3S$) states. The energy levels E can be again presented as an expansion (10). However, in this case, for $k \geq 1$, the coefficients ϵ_k differ for the singlet and triplet states, while $\epsilon_0 = -(1 + n^{-2})$. The first-order correction $\Delta E^{(1)}$ contains contributions of the Coulomb direct and exchange integrals

$$\Delta E^{(1)} = J \pm K, \quad (14)$$

$$J = 2\pi\alpha\eta^{-1}N_{1s}^2N_{ns}\frac{1}{2\pi i}\oint_{(\eta_n^+)} dy \frac{(y + \eta_n)^n}{(y - \eta_n)^n} \times \left(-\frac{\partial}{\partial\lambda}\right) \frac{1}{\lambda^2} \langle \psi_{ns} | (V_{iy} - V_{i(\lambda+y)}) | 0 \rangle \Big|_{\lambda=2\eta}, \quad (15)$$

$$K = 2\pi\alpha\eta^{-1}N_{1s}^2N_{ns}\frac{1}{2\pi i}\oint_{(\eta_n^+)} dy \frac{(y + \eta_n)^n}{(y - \eta_n)^n} \times \left(-\frac{\partial}{\partial\lambda}\right) \frac{1}{\lambda^2} \langle \psi_{ns} | (V_{i\eta} - V_{i(\lambda+\eta)}) | 0 \rangle \Big|_{\lambda=y+\eta}. \quad (16)$$

In Eq. (14), the plus and minus signs correspond to the singlet and triplet states, respectively. The matrix elements with the Coulomb wave functions are given by Eq. (13). The splitting between the energy levels with different multiplicities is just $2K$. In Tables II and III, we present the coefficients $\epsilon_1 = Z\Delta E^{(1)}/I$ calculated for the $n^1, ^3S$ terms with $n \leq 15$. In the asymptotic limit $n \gg 1$, both coefficients ϵ_1 exhibit a similar behavior as $2n^{-2}$, because the contribution due to the exchange interaction vanishes.

4. Let us now consider the high-energy electron scattering on a hydrogen-like ion being in the ground state, which results in excitation of a K-shell electron into the bound ns state ($n \geq 2$). We shall derive formulas for differential and total cross sections of the process in the leading order of non-relativistic perturbation theory. The particular case of $n = 2$ has been studied in Refs. [20, 21]. The incident electron is characterized by the energy $E_p = \mathbf{p}^2/(2m)$ and the momentum \mathbf{p} at infinitely large distances from the nucleus, while the scattered electron possesses the energy $E_{p_1} = \mathbf{p}_1^2/(2m)$ and the asymptotic momentum \mathbf{p}_1 . The energy-conservation law implies $E_p + E_{1s} = E_{p_1} + E_{ns}$.

On the example of the $1s$ - $2s$ excitation [21], we have seen that the calculations of total cross sections performed within the framework of the Born approximation are worthwhile even in the

near-threshold domain, where the expansion with respect to the powers of the reversed energy E_p^{-1} appears to be an asymptotic series. The best agreement with the exact calculations is achieved, if one truncates the expansion with taking into account only the leading high-energy term.

For non-relativistic energies E_p within the asymptotic range $I(1 - n^{-2}) \ll E_p \ll m$, $E_{p_1} \sim E_p$ and the absolute value of the asymptotic momentum of the scattered electron is estimated as $p_1 \sim p \gg \eta$. Accordingly, one needs to calculate only the Feynman diagram depicted in Fig. 1. The wave functions of both the incident and scattered high-energy electrons can be approximated by plane waves (Born approximation). The contribution of the exchange diagram turns out to be significantly suppressed and thus negligible. Using the expressions (7)–(9), the amplitude of the process can be represented as follows

$$\mathcal{A} = 4\pi\alpha N_{1s} \frac{1}{q^2} \left(-\frac{\partial}{\partial \lambda} \right) \langle \psi_{ns} | V_{i\lambda} | \mathbf{q} \rangle \Big|_{\lambda=\eta}, \quad (17)$$

$$\langle \psi_{ns} | V_{i\lambda} | \mathbf{q} \rangle = N_{ns} \frac{\pi}{i\eta q} \left\{ \frac{(\nu^* + \eta_n)^n}{(\nu^* - \eta_n)^n} - \frac{(\nu + \eta_n)^n}{(\nu - \eta_n)^n} \right\}, \quad (18)$$

where $N_{ns}^2 = \eta_n^3/\pi$, $\nu = iq - \lambda$, and $\mathbf{q} = \mathbf{p} - \mathbf{p}_1$ is the momentum transfer. Although Eq. (18) is written in the complex form, it is a real function of the square of the momentum transfer q^2 . In the limit $q^2 \rightarrow 0$, Eq. (18) is in agreement with the expression (13). Taking the derivative with respect to λ in Eq. (17) yields

$$\mathcal{A} = 4\pi\alpha \eta^{-5} N_{1s} N_{ns} T_n(x), \quad (19)$$

$$T_n(x) = \frac{2\pi}{ix^3} \left\{ \frac{(ix - \tau_-)^{n-1}}{(ix - \tau_+)^{n+1}} - \frac{(ix + \tau_-)^{n-1}}{(ix + \tau_+)^{n+1}} \right\}, \quad (20)$$

where $x = q/\eta$ and $\tau_{\pm} = 1 \pm n^{-1}$. Note, that $T_n(x)$ is a real function depending actually on x^2 .

The differential cross section for the $1s$ - ns excitation is related to the dimensionless function (20) via

$$d\sigma_{1s}^*(ns) = \frac{\sigma_0}{Z^4} \frac{4T_n^2(x)}{\pi^2 n^3 \varepsilon} dx^2, \quad (21)$$

where $\sigma_0 = \pi a_0^2 = 87.974$ Mb. Here we have also introduced the dimensionless energy $\varepsilon = E_p/I$ of the incident electron. The energy-conservation law implies $\varepsilon = \varepsilon_1 + 1 - n^{-2}$, where $\varepsilon_1 = E_{p_1}/I$ denotes the dimensionless energy of the scattered electron. The asymptotic non-relativistic energy domain is characterized by $1 - n^{-2} \ll \varepsilon \ll 2(\alpha Z)^{-2}$.

The leading high-energy contribution to the total cross section for the excitation process is given

by

$$\sigma_{1s}^*(ns) = \frac{\sigma_0}{Z^4} Q_n(\varepsilon), \quad (n \geq 2), \quad (22)$$

$$Q_n(\varepsilon) = \frac{\varkappa_n}{n^3 \varepsilon}, \quad (23)$$

$$\begin{aligned} \varkappa_n &= \frac{8}{\pi^2} \int_0^\infty dx x T_n^2(x) \\ &= \frac{2^6}{(2n+1)!} \frac{d^{2n+1}}{dx^{2n+1}} \left[\frac{\ln x}{x^5} (x - i\tau_-)^{2n-2} \right] \Big|_{x=i\tau_+} \\ &\quad - \frac{2^7}{n!} \frac{d^n}{dx^n} \left[\frac{\ln x}{x^5} \frac{(x^2 + \tau_-^2)^{n-1}}{(x + i\tau_+)^{n+1}} \right] \Big|_{x=i\tau_+}. \end{aligned} \quad (24)$$

In Eq. (24), we have chosen the regular branch of the logarithm, which assumes real values on the upper edge of the cut made along the positive semi-axis. The universal function $Q_n(\varepsilon)$ does not depend on the nuclear charge Z and describes the excitation of states with the zeroth-order matrix element of the dipole transition [15]. The dimensionless quantity \varkappa_n , which is a function of the principal quantum number n , is presented for particular values of $n \leq 12$ in Table IV. In the limit $n \gg 1$, the coefficients \varkappa_n tend to the asymptotic value $\varkappa_n \simeq 1.798$.

Let us make a few comments:

- Due to the crossing symmetry [12], the Feynman graph depicted in Fig. 1 describes also the $1s$ - ns excitation by the high-energy positron impact. The exchange effect is absent at all. To get the amplitude for the process, one needs to make the following substitutions: $\mathbf{p} \Rightarrow -\mathbf{p}_1$, which do not alter expressions for the ionization cross section. Accordingly, Eqs. (22)–(24) are also valid for the case of the positron impact.
- Although we have considered the excitation process by the high-energy electron impact, Eqs. (22)–(24) are also valid for the case of fast projectiles with another mass M . The corresponding energy-conservation law still reads $E_p - I = E_{p_1} - I_n$, where $E_p = Mv^2/2$ and I_n is given by Eq. (3). However, now it is convenient to calibrate the energies of the incident and scattered particle by the characteristic binding energy $\tilde{I} = M(\alpha Z)^2/2$, namely, $\varepsilon = E_p/\tilde{I}$ and $\varepsilon_1 = E_{p_1}/\tilde{I}$. The dimensionless energy $\varepsilon = v^2/(\alpha Z)^2$ does not depend on the mass of the incident particle, while the energy-conservation law now implies $\varepsilon = \varepsilon_1 + \mu(1 - n^{-2})$, where $\mu = m/M$. The asymptotic energy range is characterized by $\mu(1 - n^{-2}) \ll \varepsilon \ll 2(\alpha Z)^{-2}$.
- To leading order of non-relativistic perturbation theory, the total cross section for impact excitation of helium-like ions from the ground state into the $1sns$ configuration is by a factor

2 as large as that $\sigma_{1s}^*(ns)$ for hydrogen-like ions, taking into account the number of target electrons.

5. The process of the single photoionization of a hydrogen-like ion in the ns state is described by the diagram depicted in Fig. 2. The incident photon is characterized by the momentum \mathbf{k} , the energy $\omega = |\mathbf{k}| = k$, and the polarization vector \mathbf{e} . The energy-conservation law reads $E_p = \omega - I_n$, where $E_p = \mathbf{p}^2/(2m)$ is the energy of the outgoing electron and I_n is given by Eq. (3). Accordingly, the non-relativistic photoeffect can proceed at photon energies $I_n \leq \omega \ll m$. In the dipole approximation, the non-relativistic problem can be solved analytically [22, 23, 24, 25, 26]. Using the integral representation (8) for the Coulomb wave functions (7) yields the amplitude of the process under consideration in the closed form

$$\mathcal{A}_{ns} = 4\pi\eta^{-3}N_\gamma N_{ns}N_p(1-i\xi)(\mathbf{e} \cdot \mathbf{p})\Phi_n(\xi), \quad (25)$$

$$\Phi_n(\xi) = \frac{1}{(n-1)!} \frac{d^{n-1}}{dy^{n-1}} \left[\frac{y(y+n^{-1})^n}{(y^2+\xi^{-2})^2} e^{-2\xi \cot^{-1}(y\xi)} \right] \Big|_{y=1/n}, \quad (26)$$

$$N_\gamma = \frac{1}{m} \frac{\sqrt{4\pi\alpha}}{\sqrt{2\omega}}, \quad N_{ns}^2 = \frac{\eta_n^3}{\pi}, \quad N_p^2 = \frac{2\pi\xi}{1-e^{-2\pi\xi}}, \quad (27)$$

where $\xi = \eta/p$. Here we employ the Coulomb gauge, in which $(\mathbf{e} \cdot \mathbf{k}) = 0$ and $(\mathbf{e}^* \cdot \mathbf{e}) = 1$. The dimensionless function (26) can be written as

$$\Phi_n(\xi) = \frac{e^{-2\xi \cot^{-1}(\xi/n)}}{(n^2 + \xi^2)^n} \xi^4 f_n(\xi), \quad (28)$$

where $f_n(\xi)$ for particular values of $1 \leq n \leq 9$ are presented in Table V. For large values of n , it is convenient to employ the recurrence relations between the matrix elements [22, 23, 24, 25, 26].

The total cross section reads [23, 25]

$$\sigma_{ns}^+ = \frac{\sigma_0}{Z^2} F_n(\xi), \quad n^{-2} \leq \varepsilon_\gamma \ll 2(\alpha Z)^{-2}, \quad (29)$$

$$F_n(\xi) = \frac{2^7 \pi}{3n} \frac{(1+\xi^2)\xi^8}{(1-e^{-2\pi\xi})} \frac{e^{-4\xi \cot^{-1}(\xi/n)}}{(n^2 + \xi^2)^{2n+1}} f_n^2(\xi), \quad (30)$$

where $\sigma_0 = \alpha\pi a_0^2 = 0.642$ Mb. Due to the energy-conservation law, the parameter $\xi = \eta/p$ corresponds to the dimensionless energy of the photon $\varepsilon_\gamma = \omega/I$ according to $\varepsilon_\gamma = \xi^{-2} + n^{-2}$. The universal function $F_n(\xi)$ does not depend on the nuclear charge number Z .

In the high-energy non-relativistic domain, which is characterized by $n^{-2} \ll \varepsilon_\gamma \ll 2(\alpha Z)^{-2}$, the amplitude (25) simplifies and appears as

$$\mathcal{A}_{ns} = N_\gamma N_{ns} (\mathbf{e} \cdot \mathbf{p}) \frac{8\pi\eta}{q^4} = n^{-3/2} \mathcal{A}_{1s}. \quad (31)$$

Here $\mathbf{q} = \mathbf{p} - \mathbf{k} \simeq \mathbf{p}$, because the process proceeds with a large momentum transfer $q \gg \eta$. The total cross section reads [14]

$$\sigma_{ns}^+ = \frac{\sigma_0}{Z^2} \frac{2^8}{3n^3} \xi^7 = \frac{\sigma_{1s}^+}{n^3}, \quad (32)$$

where $\xi \simeq \varepsilon_\gamma^{-1/2}$. The formula (32), which provides just the leading term in the expansion of Eq. (29) with respect to the parameter $\xi \ll 1$, can be obtained within the Born approximation. Since the function (30) involves also the parameter $\pi\xi$, which originates from the normalization factor of the Coulomb wave function of the continuous spectrum, the convergence of the ξ expansion is sufficiently slow. Note also that, since the electron-nucleus binding for the excited ns electron is weaker than that for the K-shell electron, the cross section σ_{ns}^+ is suppressed by the factor of n^{-3} with respect to the cross section σ_{1s}^+ . In the limiting case of a free electron, the cross section for single photoeffect tends to zero [12].

6. Let us consider the single ionization of helium-like ions in the $1sns(^1,^3S)$ states by high-energy photon impact, which is not followed by excitation of the target. The principal quantum number n is assumed to be $n \geq 2$. For the ground state, the problem has been studied in Ref. [27]. The process can proceed by two different channels. We shall start with ionization of the K-shell electron. Neglecting the electron-electron interaction, the amplitude of the process reads

$$\mathcal{A}_I^{(0)} = \mathcal{A}_{1s}, \quad (33)$$

where \mathcal{A}_{1s} is given by Eq. (31). The total cross section is just σ_{1s}^+ given by Eq. (32), that is, it keeps the same form for both the singlet and triplet states. The spin dependence appears, when one takes into account the electron-electron interaction.

In first-order perturbation theory, the amplitude for the first ionization channel is $\mathcal{A}_I = \mathcal{A}_I^{(0)} + \mathcal{A}_I^{(1)}$. Within the high-energy asymptotic domain, the dominant contribution to the correlation correction $\mathcal{A}_I^{(1)}$ arises only from the diagrams depicted in Figs. 3(a) and (b), while the other

diagrams can be neglected. In explicit terms, one can write

$$\mathcal{A}_I^{(1)} = \mathcal{A}_a^{(1)} \pm \mathcal{A}_b^{(1)}, \quad (34)$$

$$\begin{aligned} \mathcal{A}_a^{(1)} = & \alpha N_\gamma N_{1s} (\mathbf{e} \cdot \mathbf{p}) \frac{\eta_n}{n^2} \frac{1}{(2\pi i)^2} \oint \prod_{k=1}^{(\eta_n^+)_2} \left[dy_k \frac{(y_k + \eta_n)^n}{(y_k - \eta_n)^n} \right] \\ & \times \left(-\frac{\partial}{\partial \lambda} \right) \frac{1}{\lambda^2} \langle \mathbf{q} | G_R(E_{1s}) (V_{i\eta} - V_{i(\lambda+\eta)}) | 0 \rangle \Big|_{\lambda=y_1+y_2}, \end{aligned} \quad (35)$$

$$\begin{aligned} \mathcal{A}_b^{(1)} = & \alpha N_\gamma N_{1s} (\mathbf{e} \cdot \mathbf{p}) \frac{\eta_n}{n^2} \frac{1}{(2\pi i)^2} \oint \prod_{k=1}^{(\eta_n^+)_2} \left[dy_k \frac{(y_k + \eta_n)^n}{(y_k - \eta_n)^n} \right] \\ & \times \left(-\frac{\partial}{\partial \lambda} \right) \frac{1}{\lambda^2} \langle \mathbf{q} | G_R(E_{1s}) (V_{iy_2} - V_{i(\lambda+y_2)}) | 0 \rangle \Big|_{\lambda=y_1+\eta}. \end{aligned} \quad (36)$$

Here again the momentum transfer is $\mathbf{q} = \mathbf{p} - \mathbf{k} \simeq \mathbf{p}$. In the derivation, we have used the Born approximation for the wave function of the ejected high-energy electron. In Eq. (34), the plus and minus signs correspond to the singlet and triplet states, respectively. For $q \gg \eta$, the matrix element involving the reduced Coulomb Green's function $G_R(E_{1s})$ was evaluated in the work [27].

The correlation corrections for the amplitude can be cast into the following form

$$\mathcal{A}_I^{(1)} = N_\gamma N_{1s} \frac{4\pi\eta}{Zq^4} (\mathbf{e} \cdot \mathbf{p}) a_1^\pm. \quad (37)$$

The coefficients a_1^\pm , which correspond to the singlet and triplet states, are presented in Tables VI and VII. In the limit $n \gg 1$, the product $n^3 a_1^+$ tends to the asymptotic constant -1.031 , while $n^3 a_1^-$ approaches the value 0.087 . Employing Eqs. (33) and (37) yields the total amplitude for the single K-shell photoeffect

$$\mathcal{A}_I = \mathcal{A}_I^{(0)} + \mathcal{A}_I^{(1)} = \mathcal{A}_I^{(0)} \left(1 + \frac{a_1^\pm}{2Z} \right), \quad (38)$$

which takes into account the electron correlations. The ionization cross section reads

$$\sigma_I^+ = \sigma_{1s}^+ (1 + a_1^\pm Z^{-1}), \quad (39)$$

where σ_{1s}^+ is given by Eq. (32). As it is seen, account of the electron-electron interaction gives rise to the significant dependence of ionization cross sections on the spin multiplicity of atomic states. Indeed, the characteristic orbits of the $1s$ and ns electrons are somewhat different. However, in the singlet state, both electrons are allowed to be at the same spatial point, while, in the triplet state, it is forbidden by the Pauli principle. Accordingly, in the n^1S state, the account of the dominant correlation corrections attenuates the binding of the K-shell electron with the nucleus. As a result, the cross section decreases in comparison with the single-particle prediction (32). In the

n^3S state, the correlation corrections amplify the electron-nucleus binding for the K-shell electron, what makes the ionization cross section σ_I^+ even a bit larger than σ_{1s}^+ .

Another channel for the single photoeffect on helium-like ions in the $1sns$ (1^3S) states is ionization of the ns electron. To leading order, the amplitude of the process reads

$$\mathcal{A}_{\text{II}}^{(0)} = \mathcal{A}_{ns}, \quad (40)$$

where \mathcal{A}_{ns} is given by Eq. (31). The total cross section coincides with the formula (32), being independent of the spin multiplicity of the wave functions.

To first order of the perturbation theory with respect to the electron-electron interaction, one needs to take into account the diagrams drawn in Figs. 3(c) and (d). The corresponding contributions can be represented as

$$\begin{aligned} \mathcal{A}_c^{(1)} &= 2\alpha \eta^2 N_\gamma N_{ns} (\mathbf{e} \cdot \mathbf{p}) \frac{1}{2\pi i} \oint_{(\eta_n^+)} dy \frac{(y + \eta_n)^n}{(y - \eta_n)^n} \\ &\times \left(-\frac{\partial}{\partial \lambda} \right) \frac{1}{\lambda^2} \langle \mathbf{q} | G_R(E_{ns}) (V_{iy} - V_{i(\lambda+y)}) | 0 \rangle \Big|_{\lambda=2\eta}, \end{aligned} \quad (41)$$

$$\begin{aligned} \mathcal{A}_d^{(1)} &= 2\alpha \eta^2 N_\gamma N_{ns} (\mathbf{e} \cdot \mathbf{p}) \frac{1}{2\pi i} \oint_{(\eta_n^+)} dy \frac{(y + \eta_n)^n}{(y - \eta_n)^n} \\ &\times \left(-\frac{\partial}{\partial \lambda} \right) \frac{1}{\lambda^2} \langle \mathbf{q} | G_R(E_{ns}) (V_{i\eta} - V_{i(\lambda+\eta)}) | 0 \rangle \Big|_{\lambda=y+\eta}. \end{aligned} \quad (42)$$

Here the matrix elements should be evaluated with the reduced Green's function $G_R(E_{ns})$ at the energy point $E_{ns} = -\eta_n^2/(2m)$, which is related to the usual non-relativistic Green's function $G(E)$ via

$$G_R(E_{ns}) = \lim_{E \rightarrow E_{ns}} \left\{ G(E) - \frac{|\psi_{ns}\rangle \langle \psi_{ns}|}{E - E_{ns}} \right\}. \quad (43)$$

For $q \gg \eta$, the Coulomb matrix element has the following integral representation [19]

$$\langle \mathbf{q} | G(E) V_{i\lambda} | 0 \rangle \simeq 2^5 \pi m \eta \frac{ip_1}{q^4} \int_0^1 \frac{t^{-i\zeta} dt}{[\lambda - ip_1 - (\lambda + ip_1)t]^2}, \quad (44)$$

where $\zeta = \eta/p_1$ and $p_1 = \sqrt{2mE}$ is the intermediate momentum. Performing the analytical continuation of Eq. (44) and canceling the pole terms according to the definition (43) yield

$$\begin{aligned} \langle \mathbf{q} | G_R(E_{ns}) V_{i\lambda} | 0 \rangle &= 2^5 \pi m \frac{\eta^2}{q^4} \left\{ P_n(\lambda) + \right. \\ &\left. + (n+1)(\lambda - \eta_n)^n \int_0^1 \frac{\ln t dt}{[\lambda(1-t) + \eta_n(1+t)]^{n+2}} \right\}. \end{aligned} \quad (45)$$

The explicit expressions of the function $P_n(\lambda)$ for particular values of $n \leq 9$ are given in Table VIII.

In the case of ionization of the ns electron, it is convenient to introduce the correlation coefficients b_1^\pm according to

$$\mathcal{A}_{\text{II}}^{(1)} = \mathcal{A}_{\text{c}}^{(1)} \pm \mathcal{A}_{\text{d}}^{(1)} = N_\gamma N_{ns} \frac{4\pi\eta}{Zq^4} (\mathbf{e} \cdot \mathbf{p}) b_1^\pm, \quad (46)$$

where plus and minus correspond to the singlet and triplet states, respectively. The coefficients b_1^\pm are evaluated in Tables IX and X. In the asymptotic limit $n \gg 1$, b_1^+ tends to the constant -1.47 , while b_1^- approaches to the value -2.44 . The total amplitude for ionization of the ns electron is $\mathcal{A}_{\text{II}} = \mathcal{A}_{\text{II}}^{(0)} + \mathcal{A}_{\text{II}}^{(1)}$. The partial cross section for the second channel reads

$$\sigma_{\text{II}}^+ = \sigma_{ns}^+ (1 + b_1^\pm Z^{-1}), \quad (47)$$

where σ_{ns}^+ is given by Eq. (32). As it is seen, account of the electron-electron interaction turns out to be crucial for describing the high-energy photoeffect on the ns electron. Especially, it concerns the triplet states, where the screening corrections b_1^- are very large. Due to the Pauli exclusion principle, the transfer of a large momentum from the nucleus to the ns electron appears to be hardly probable. Accordingly, the ionization cross section strongly decreases in comparison with the single-particle approximation (32). Note that, for a neutral helium atom in the n^3S state, Eq. (47) predicts negative values for σ_{II}^+ , if $n \geq 3$. In this case, one needs to take into account higher-order correlation corrections, which have not been considered in the present paper. For two-electron ions with $Z \geq 3$, the cross section (47) is always positive.

Taking into account both ionization channels, the total cross section for the single photoeffect on helium-like ions in the $1sns$ ($1,^3S$) states reads

$$\sigma^+ = \sigma_{\text{I}}^+ + \sigma_{\text{II}}^+ \quad (48)$$

$$= \sigma_{1s}^+ (1 + a_1^\pm Z^{-1}) + \sigma_{ns}^+ (1 + b_1^\pm Z^{-1}). \quad (49)$$

In view of the relation (32), Eq. (49) can be also cast into the following form

$$\sigma^+ = \sigma_{1s}^+ \{1 + n^{-3} + (a_1^\pm + n^{-3} b_1^\pm) Z^{-1}\}. \quad (50)$$

The coefficients a_1^\pm and b_1^\pm describe the dominant contribution to the correlation effect at high photon energies.

Although the expressions (49) and (50) have been derived within the Born approximation, Eq. (49) can be employed for a sufficiently wide energy domain, provided the single-particle cross sections are described by Eq. (29) [27, 28]. Indeed, the expression (29) keeps the same form to first order of the perturbation theory, taking into account the correlation corrections to the

binding energy. However, for the high-energy domain characterized by $\varepsilon_\gamma^{-1} \ll \xi \ll 1$, the binding energy corrections are negligibly small with respect to the photon energy. Since the function (30) involves the correct dependence on the parameter ξ , Eq. (49) turns out to be also correct, neglecting terms of the order of about $(\xi/Z)^2 = (m\alpha/p)^2$ (see also extensive discussions on this topic in Refs. [29, 30, 31, 32]). In this paper, we have omitted some correlation corrections to the amplitude, which are of about $m\alpha/p$ (in particular, those, which arise due to the final-state interaction). However, the neglected terms are purely imaginary and do not contribute to the ionization cross section.

Concluding, we have investigated the processes of excitation and ionization of light multicharged ions by impact of high-energy particles, which proceed with participation of the ns electrons. The dominant correlation corrections to the energy levels and photoionization cross sections are calculated analytically within the framework of non-relativistic perturbation theory. As major result, the universal scalings for the excitation and ionization cross sections are deduced.

Acknowledgments

The authors acknowledge financial support from BMBF, DFG, GSI, and INTAS (Grant no. 06-1000012-8881).

TABLE I: For the pure $ns^2(^1S)$ states of helium-like ions, the dimensionless coefficients ϵ_1 are tabulated according to Eq. (12).

n	$n^2\epsilon_1$		n	$n^2\epsilon_1$	
	analytical	numerical		analytical	numerical
1 5/4		1.25	9 2555635959/2147483648		1.19006
2 77/64		1.20313	10 40886039491/34359738368		1.18994
3 153/128		1.19531	11 81765970991/68719476736		1.18985
4 19541/16384		1.19269	12 10465450564505/8796093022208		1.18978
5 39043/32768		1.19150	13 20929978151879/17592186044416		1.18973
6 624353/524288		1.19086	14 334867944396713/281474976710656		1.18969
7 1248305/1048576		1.19048	15 669717016529889/562949953421312		1.18966
8 1277999141/1073741824		1.19023	16 5486195355159701189/4611686018427387904		1.18963

TABLE II: For the $1sns(^1S)$ terms of helium-like ions, the dimensionless coefficients ϵ_1 are tabulated according to Eqs. (14)–(16).

n	$n^2\epsilon_1$	
	analytical	numerical
2 1352/729		1.8546
3 31041/16384		1.8946
4 18741536/9765625		1.9191
5 87737225/45349632		1.9347
6 1319346413640/678223072849		1.9453
7 137428433691773/70368744177664		1.9530
8 294001828174792832/150094635296999121		1.9588
9 12270688433717907483/6250000000000000000		1.9633
10 160115079305309345784200/81402749386839761113321		1.9669
11 19575441723611998332463421/9937105900423855516680192		1.9699
12 180937160122853564881284932640/91733330193268616658399616009		1.9724
13 7619039446472988471652076553139/3858646740351497994569680683008		1.9745
14 8421485561700554490032347126878248/4261134649619646370410919189453125		1.9763
15 168262776200010701611816602447746396925/85070591730234615865843651857942052864		1.9779

TABLE III: For the $1sns(^3S)$ terms of helium-like ions, the dimensionless coefficients ϵ_1 are tabulated according to Eqs. (14)–(16).

n	$n^2\epsilon_1$	
	analytical	numerical
2	1096/729	1.5034
3	27639/16384	1.6869
4	17279264/9765625	1.7694
5	41200175/22674816	1.8170
6	1253464471368/678223072849	1.8482
7	131602743884003/70368744177664	1.8702
8	283169102583793792/150094635296999121	1.8866
9	1483842517395327999/781250000000000000	1.8993
10	155435328837703659864200/81402749386839761113321	1.9095
11	19056793993685438861087899/9937105900423855516680192	1.9177
12	176552744806540188413776122912/91733330193268616658399616009	1.9246
13	3724467497547548854690865614181/1929323370175748997284840341504	1.9304
14	8247164359458263840860888961901352/4261134649619646370410919189453125	1.9354
15	165016222122028120626234494334313260675/85070591730234615865843651857942052864	1.9398

TABLE IV: For various values of the principal quantum number n , the dimensionless coefficients \varkappa_n are calculated according to Eq. (24).

n	\varkappa_n	
	analytical	numerical
2	1048576/295245	3.5515
3	85293/35840	2.3798
4	806380109824/384521484375	2.0971
5	2815390625/1420541793	1.9819
6	2238980830283169792/1164315722505971035	1.9230
7	835179111639733/442209832796160	1.8886
8	156418330091764719082799104/83789232212292561749679885	1.8668
9	10197593930567041902351/5506157875061035156250	1.8520
10	580608990927250169145671680000000/315279866676074279955576140196657	1.8416
11	28550108411751156734369151319/15568186626467172764709027840	1.8339
12	9784817930963041730702096023760230416384/5352585600085746305433457063492098280775	1.8280

TABLE V: For various values of the principal quantum number n , the dimensionless functions $f_n(\xi)$ are tabulated according to Eqs. (26) and (28).

n	$f_n(\xi)$
1	$2/(1 + \xi^2)$
2	32
3	$54(27 + 7\xi^2)$
4	$(512/3)(768 + 288\xi^2 + 23\xi^4)$
5	$(1250/3)(46875 + 20625\xi^2 + 2545\xi^4 + 91\xi^6)$
6	$(864/5)(25194240 + 12130560\xi^2 + 1827360\xi^4 + 105552\xi^6 + 2023\xi^8)$
7	$(4802/45)(12711386205 + 6485401125\xi^2 + 1097665170\xi^4 + 79704282\xi^6 + 2547265\xi^8 + 29233\xi^{10})$
8	$(8192/315)(21646635171840 + 11499774935040\xi^2 + 2101597962240\xi^4 + 175037743104\xi^6 + 7190401024\xi^8 + 140890496\xi^{10} + 1044871\xi^{12})$
9	$(4374/35)(2402063207770905 + 1314709492319055\xi^2 + 253715866938765\xi^4 + 23169940624971\xi^6 + 1109810543211\xi^8 + 28441442925\xi^{10} + 366767919\xi^{12} + 1859129\xi^{14})$

TABLE VI: For the $1sns(^1S)$ terms of helium-like ions, the dimensionless coefficients a_1^+ are tabulated according to Eqs. (34)–(37).

n	$n^3 a_1^+$	
	analytical	numerical
2	$(8/2187)(-1679 + 3360 \ln(3/2))$	-1.1582
3	$(81/131072)(-24245 + 78184 \ln(4/3))$	-1.0832
4	$(192/48828125)(-7097629 + 30599840 \ln(5/4))$	-1.0596
5	$(125/3265173504)(-1171956731 + 6277663800 \ln(6/5))$	-1.0491
6	$(648/23737807549715)(-2411780852069 + 15397639065760 \ln(7/6))$	-1.0435
7	$(1029/5629499534213120)(-496846568524997 + 3678208705153360 \ln(8/7))$	-1.0401
8	$(512/47279810118554723115)(-11062929106398468157 + 93112579989061637760 \ln(9/8))$	-1.0379
9	$(729/35000000000000000000)(-733561568265485829193 + 6915165610828616935920 \ln(10/9))$	-1.0365

TABLE VII: For the $1sns(^3S)$ terms of helium-like ions, the dimensionless coefficients a_1^- are tabulated according to Eqs. (34)–(37).

n	$n^3 a_1^-$	
	analytical	numerical
2	$(8/2187)(-1399 + 3552 \ln(3/2))$	0.1507
3	$(27/131072)(-67801 + 237576 \ln(4/3))$	0.1123
4	$(64/48828125)(-20509663 + 92256480 \ln(5/4))$	0.1006
5	$(125/1632586752)(-572430899 + 3146517000 \ln(6/5))$	0.0955
6	$(216/4747561509943)(-1424070240731 + 9251393817120 \ln(7/6))$	0.0927
7	$(2401/5629499534213120)(-210463375781159 + 1577733920822640 \ln(8/7))$	0.0911
8	$(512/6754258588364960445)(-1566435008617827011 + 13309413901475690880 \ln(9/8))$	0.0901
9	$(729/4375000000000000000)(-91055968618569041179 + 864741335682205139760 \ln(10/9))$	0.0893

TABLE VIII: For various values of the principal quantum number n , the functions $P_n(\lambda)$ are tabulated according to Eq. (45).

n	$P_n(\lambda)$
1	$\frac{2\eta}{(\eta + \lambda)^3} - \frac{5}{2(\eta + \lambda)^2}$
2	$\frac{1}{8\eta_2^2} - \frac{3\lambda^2}{(\lambda + \eta_2)^4} - \frac{\lambda}{2(\lambda + \eta_2)^3} + \frac{5}{4(\lambda + \eta_2)^2}$
3	$\frac{\lambda}{24\eta_3^3} - \frac{16\lambda^3}{3(\lambda + \eta_3)^5} + \frac{14\lambda}{3(\lambda + \eta_3)^3} - \frac{5}{3(\lambda + \eta_3)^2}$
4	$\frac{\lambda^2}{64\eta_4^4} - \frac{\lambda}{48\eta_4^3} + \frac{5}{192\eta_4^2} - \frac{10\lambda^4}{(\lambda + \eta_4)^6} + \frac{7\lambda^3}{3(\lambda + \eta_4)^5} + \frac{13\lambda^2}{(\lambda + \eta_4)^4} - \frac{39\lambda}{4(\lambda + \eta_4)^3} + \frac{47}{24(\lambda + \eta_4)^2}$
5	$\frac{\lambda^3}{160\eta_5^5} - \frac{\lambda^2}{64\eta_5^4} + \frac{\lambda}{60\eta_5^3} + \frac{1}{192\eta_5^2} - \frac{96\lambda^5}{5(\lambda + \eta_5)^7} + \frac{148\lambda^4}{15(\lambda + \eta_5)^6} + \frac{472\lambda^3}{15(\lambda + \eta_5)^5} - \frac{38\lambda^2}{(\lambda + \eta_5)^4} + \frac{232\lambda}{15(\lambda + \eta_5)^3} - \frac{131}{60(\lambda + \eta_5)^2}$
6	$\frac{\lambda^4}{384\eta_6^6} - \frac{3\lambda^3}{320\eta_6^5} + \frac{13\lambda^2}{960\eta_6^4} - \frac{7\lambda}{960\eta_6^3} + \frac{17}{1920\eta_6^2} - \frac{112\lambda^6}{3(\lambda + \eta_6)^8} + \frac{464\lambda^5}{15(\lambda + \eta_6)^7} + \frac{208\lambda^4}{3(\lambda + \eta_6)^6} - \frac{368\lambda^3}{3(\lambda + \eta_6)^5} + \frac{229\lambda^2}{3(\lambda + \eta_6)^4} - \frac{65\lambda}{3(\lambda + \eta_6)^3} + \frac{71}{30(\lambda + \eta_6)^2}$
7	$\frac{\lambda^5}{896\eta_7^7} - \frac{\lambda^4}{192\eta_7^6} + \frac{67\lambda^3}{6720\eta_7^5} - \frac{3\lambda^2}{320\eta_7^4} + \frac{71\lambda}{13440\eta_7^3} + \frac{1}{240\eta_7^2} - \frac{512\lambda^7}{7(\lambda + \eta_7)^9} + \frac{2992\lambda^6}{35(\lambda + \eta_7)^8} + \frac{4944\lambda^5}{35(\lambda + \eta_7)^7} - \frac{2476\lambda^4}{7(\lambda + \eta_7)^6} + \frac{2104\lambda^3}{7(\lambda + \eta_7)^5} - \frac{129\lambda^2}{(\lambda + \eta_7)^4} + \frac{989\lambda}{35(\lambda + \eta_7)^3} - \frac{353}{140(\lambda + \eta_7)^2}$
8	$\frac{\lambda^6}{2048\eta_8^8} - \frac{5\lambda^5}{1792\eta_8^7} + \frac{289\lambda^4}{43008\eta_8^6} - \frac{29\lambda^3}{3360\eta_8^5} + \frac{457\lambda^2}{71680\eta_8^4} - \frac{53\lambda}{26880\eta_8^3} + \frac{919}{215040\eta_8^2} - \frac{144\lambda^8}{(\lambda + \eta_8)^{10}} + \frac{7704\lambda^7}{35(\lambda + \eta_8)^9} + \frac{1328\lambda^6}{5(\lambda + \eta_8)^8} - \frac{4722\lambda^5}{5(\lambda + \eta_8)^7} + \frac{1032\lambda^4}{(\lambda + \eta_8)^6} - \frac{1193\lambda^3}{2(\lambda + \eta_8)^5} + \frac{984\lambda^2}{5(\lambda + \eta_8)^4} - \frac{1407\lambda}{40(\lambda + \eta_8)^3} + \frac{1487}{560(\lambda + \eta_8)^2}$
9	$\frac{\lambda^7}{4608\eta_9^9} - \frac{3\lambda^6}{2048\eta_9^8} + \frac{275\lambda^5}{64512\eta_9^7} - \frac{99\lambda^4}{14336\eta_9^6} + \frac{17\lambda^3}{2520\eta_9^5} - \frac{279\lambda^2}{71680\eta_9^4} + \frac{523\lambda}{322560\eta_9^3} + \frac{207}{71680\eta_9^2} - \frac{2560\lambda^9}{9(\lambda + \eta_9)^{11}} + \frac{56864\lambda^8}{105(\lambda + \eta_9)^{10}} + \frac{141952\lambda^7}{315(\lambda + \eta_9)^9} - \frac{107168\lambda^6}{45(\lambda + \eta_9)^8} + \frac{48416\lambda^5}{15(\lambda + \eta_9)^7} - \frac{21236\lambda^4}{9(\lambda + \eta_9)^6} + \frac{46952\lambda^3}{45(\lambda + \eta_9)^5} - \frac{1402\lambda^2}{5(\lambda + \eta_9)^4} + \frac{13348\lambda}{315(\lambda + \eta_9)^3} - \frac{6989}{2520(\lambda + \eta_9)^2}$

TABLE IX: For the $1sns(^1S)$ terms of helium-like ions, the dimensionless coefficients b_1^+ are tabulated according to Eqs. (41), (42), and (46).

n	b_1^+	
	analytical	numerical
2 (4/2187)(-772 + 159 ln 3)		-1.0925
3 (3/131072)(-73875 + 13816 ln 4)		-1.2525
4 (72/48828125)(-1248684 + 219365 ln 5)		-1.3207
5 (5/3265173504)(-1268946065 + 213266808 ln 6)		-1.3580
6 (12/23737807549715)(-3996048740304 + 649245311015 ln 7)		-1.3814
7 (7/5629499534213120)(-1674319803898931 + 264724373084400 ln 8)		-1.3974
8 (16/47279810118554723115)(-6304966995252184568 + 974522181024852075 ln 9)		-1.4090
9 (9/35000000000000000000)(-847067488481686729599 + 128414477117971809520 ln 10)		-1.4178

TABLE X: For the $1sns(^3S)$ terms of helium-like ions, the dimensionless coefficients b_1^- are tabulated according to Eqs. (41), (42), and (46).

n	b_1^-	
	analytical	numerical
2 (4/2187)(-1604 + 543 ln 3)		-1.8426
3 (3/131072)(-146181 + 41032 ln 4)		-2.0439
4 (8/48828125)(-22143244 + 5629965 ln 5)		-2.1434
5 (5/1632586752)(-1254848345 + 298760904 ln 6)		-2.2037
6 (12/4747561509943)(-1589311619664 + 360435860155 ln 7)		-2.2444
7 (21/5629499534213120)(-1116056979027599 + 243593185902000 ln 8)		-2.2737
8 (16/6754258588364960445)(-1810645396585286728 + 382953780229600125 ln 9)		-2.2959
9 (9/43750000000000000000)(-213879211569028496997 + 44048190258616320560 ln 10)		-2.3133

-
- [1] B.H. Bransden, M.R.C. McDowell, Phys. Rep. 46 (1978) 249.
 - [2] R.J.W. Henry, Phys. Rep. 68 (1981) 1.
 - [3] Y. Itikawa, Phys. Rep. 143 (1986) 69.
 - [4] H. Knudsen, J.F. Reading, Phys. Rep. 212 (1992) 107.
 - [5] Y. Itikawa, Atomic Data Nucl. Data Tables 63 (1996) 315.
 - [6] V.I. Fisher, Y.V. Ralchenko, V.A. Bernshtam, A. Goldgirsh, Y. Maron, L.A. Vainshtein, I. Bray, H. Golten, Phys. Rev. A 55 (1997) 329.
 - [7] J. Eichler, Th. Stöhlker, Phys. Rep. 439 (2007) 1.
 - [8] A.I. Mikhailov, I.A. Mikhailov, A.V. Nefiodov, G. Plunien, G. Soff, Pis'ma Zh. Eksp. Teor. Fiz. 78 (2003) 141, JETP Lett. 78 (2003) 110.
 - [9] A.I. Mikhailov, I.A. Mikhailov, A.V. Nefiodov, G. Plunien, Phys. Lett. A 355 (2006) 363.
 - [10] A.I. Mikhailov, A.V. Nefiodov, G. Plunien, Phys. Rev. Lett. 97 (2006) 233003.
 - [11] A.V. Nefiodov, G. Plunien, Phys. Lett. A 363 (2007) 115.
 - [12] V.B. Berestetskii, E.M. Lifshits, L.P. Pitaevskii, Quantum Electrodynamics (2nd ed.), Pergamon Press, London, 1982.
 - [13] The use of the same notations for the electron mass and projection of the orbital angular momentum is not confusing, because the latter is related with the angular dependence of wave functions only.
 - [14] H.A. Bethe, E.E. Salpeter, Quantum Mechanics of One- and Two-Electron Atoms, Plenum, New York, 1977.
 - [15] L.D. Landau, E.M. Lifshits, Quantum Mechanics: Non-relativistic Theory, third ed., Pergamon Press, London, 1977.
 - [16] C. Sinha, N. Roy, N.C. Sil, J. Phys. B 11 (1978) 1807.
 - [17] C. Sinha, N.C. Sil, J. Phys. B 12 (1979) 1711.
 - [18] A.K. Das, N.C. Sil, J. Phys. B 17 (1984) 3987.
 - [19] M.Ya. Amusia, A.I. Mikhailov, Zh. Eksp. Teor. Fiz. 111 (1997) 862, JETP 84 (1997) 474.
 - [20] V.M. Galitskii, B.M. Karnakov, V.I. Kogan, Problems in quantum mechanics, Nauka, Moscow, 1992.
 - [21] A.V. Nefiodov, G. Plunien, Phys. Lett. A (2007), doi:10.1016/j.physleta.2007.06.053.
 - [22] W. Gordon, Ann. Phys. (Leipzig) 2 (1929) 1031.
 - [23] M. Stobbe, Ann. Phys. (Leipzig) 7 (1930) 661.
 - [24] L.C. Biedenharn, J.L. McHale, R.M. Thaler, Phys. Rev. 100 (1955) 376.
 - [25] A. Burgess, Mem. Roy. Astron. Soc. 69 (1965) 1.
 - [26] G. Soff, J. Rafelski, Z. Phys. D 14 (1989) 187.
 - [27] A.I. Mikhailov, A.V. Nefiodov, G. Plunien, Phys. Lett. A 358 (2006) 211.
 - [28] A.I. Mikhailov, A.V. Nefiodov, G. Plunien, Phys. Lett. A 368 (2007) 391.
 - [29] T. Surić, E.G. Drukarev, R.H. Pratt, Zh. Eksp. Teor. Fiz. 124 (2003) 243, JETP 97 (2003) 217.

- [30] T. Surić, E.G. Drukarev, R.H. Pratt, Phys. Rev. A 67 (2003) 022709; *ibid.* 67 (2003) 059902, Erratum.
- [31] T. Surić, R.H. Pratt, J. Phys. B 37 (2004) L93.
- [32] T. Surić, Rad. Phys. Chem. 70 (2004) 253.

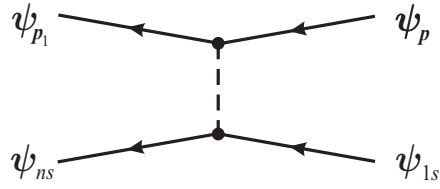


FIG. 1: Feynman diagram for excitation of a K-shell electron into the bound ns state by electron impact. Solid lines denote electrons in the external Coulomb field of the nucleus, while the dashed line denotes the electron-electron Coulomb interaction.

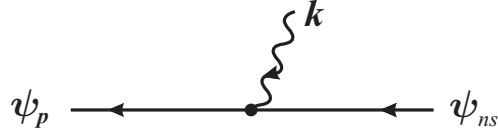


FIG. 2: Feynman diagram for ionization of the bound ns electron by photon impact.

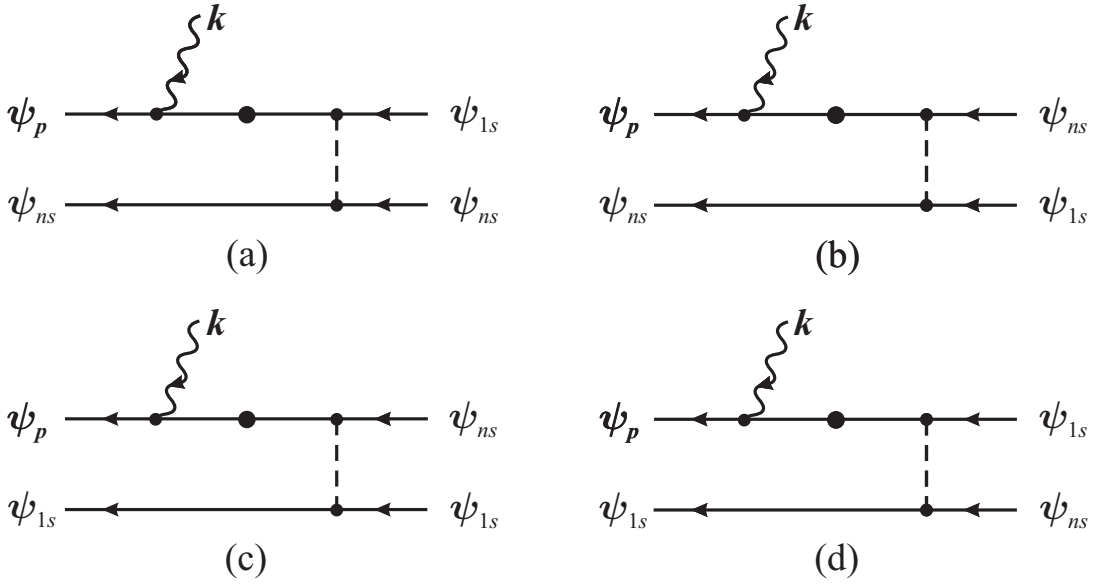


FIG. 3: Feynman diagrams for single ionization of helium-like ion in the $1sns$ configurations following by the absorption of a high-energy photon. The lines with a heavy dot correspond to the reduced Coulomb Green's functions. The diagrams (a) and (b) describe ionization of the K-shell electron, while diagrams (c) and (d) describe ionization of the ns electron.